[11]Chang, J. W., and Park, S. O., "Measurements in the Tip Vortex Roll-Up Region of an Oscillating Wing," *AIAA Journal*, Vol. 38, No. 6, 2000, pp. 1092–1095.

[12]Muller, T. J., and Batill, S. M., "Experimental Studies of Separation on a Two-Dimensional Airfoil at Low Reynolds Number," *AIAA Journal*, Vol. 20, No. 4, 1982, pp. 457–463.

Visualized Vortices on Unmanned Combat Air Vehicle Planform: Effect of Reynolds Number

M. Elkhoury* and D. Rockwell†
Lehigh University, Bethlehem, Pennsylvania 18015

I. Introduction

FLOW past an aerodynamic planform at angle of attack generates complex flow patterns due to abrupt changes in sweep angle and to the existence of a wing root. Such planforms generate more than one vortex system. For example, one type of vortex arises from the main fuselage or strake, and another emanates at the wing root. Generally speaking, these vortices can interact with one another. Previous investigations have clearly demonstrated that the development and potential interaction of vortices is a function of Reynolds number. Hebbar et al.[1] characterize the Reynolds number dependence of the vortices on a double delta wing planform. They employ dye visualization, along with laser Doppler velocimetry, to determine details of the flow patterns. Their dye visualization showed a strong dependence on Reynolds number of the onset of vortex breakdown, as well as the interaction of the vortices. At a lower value of Reynolds number, the vortices from the apex of the wing and the wing root interacted with each other, whereas at a higher value, they developed nearly parallel to one another, and their axes did not intersect. Furthermore, the angle of inclination of the wing root vortex changed substantially with Reynolds number. Verhaagen[2] provides an overview of investigations that show similar features of the vortex development and interaction as a function of Reynolds number. His overview also includes oil-film visualization for determination of the corresponding patterns of surface shear stress lines as a function of Reynolds number. Further investigations on the effects of Reynolds number have focused on relatively high values extending from 0.5 to 2.5×10^6, as described by Visser and Washburn[3] and Verhaagen et al.[4] These investigations also included variations of angle of attack. Visser and Washburn[3] focused on the boundary-layer transition on delta wings having a flat surface on the leeward side. The occurrence of transition involved outward movement of the secondary separation line. Furthermore, it was found that the occurrence of transition was strongly correlated with the strength of the vortex, as represented by its circulation evaluated in the crossflow plane. Verhaagen et al.[4] characterized the effect of Reynolds number on the surface pressure coefficient along the leeward surface of the wing and, furthermore, showed the effect of Reynolds number on qualitative visualization, as well as on topological representations of the surface flow patterns.

Unmanned combat air vehicle (UCAV) planforms typically involve relatively low values of sweep angle of both the fuselage (main body) and the wing extension. Little attention has been devoted to understanding the flow structure on simple delta wings of low sweep angle, let alone more complex configurations such as UCAV planforms. The general issue, therefore, arises as to the dependence of the flow patterns on a UCAV on both the Reynolds number and the angle of attack. The aim of the present investigation is to provide various measures of the visualized dye patterns, including the degree of interaction of vortices, the onset of vortex breakdown, and the effective sweep angle of the wing root vortex, as a function of both Reynolds number and angle of attack.

II. Experimental System and Techniques

Experiments were performed in a large-scale water channel, with a test section 927 mm wide, 610 mm deep, and 4928 mm long. The flow velocity was varied over the range of 27–214 mm/s. The chord of the planform was $C = 188$ mm, and, therefore, values of Reynolds number Re based on chord ranged from $Re = 5 \times 10^3$ to 4×10^4.

The planform approximated the Boeing X-45 UCAV. An outline of this planform is given in Fig. 1. The wing had a thickness of 3.2 mm and was beveled on its windward side at an angle of 30 deg. The wing was held in position by a streamlined strut of thickness 2.5 mm. Extensive visualization in conjunction with particle image velocimetry ascertained that the position of this strut did not have an effect on the flow patterns on the leeward surface of the wing. Dye ports were located near the tip of the apex of the wing, that is, at a distance of 2.0 mm from the tip, with the openings on the leeward surface.

Similarly, ports were located at the wing root. By allowing dye to flow simultaneously from these four ports, it was possible to examine simultaneously the overall symmetry of the patterns, as well as the degree of interaction of the vortex systems. The wing was mounted at negative angle of attack, with the bevel on the windward surface, such that images of the dye could be recorded by a camera oriented such that its viewing axis extended upward through the bottom surface of the water channel. This high-resolution charge-coupled device (CCD) camera had an array of 1024×1024 pixels, of which 1008×1016 were light sensitive. Images were recorded at a rate of 30 frames per second. Representative excerpts from the visualization sequences are shown herein.

III. Overview of Visualized Patterns

Figures 2a and 2b show patterns of dye visualization, over a Reynolds number range of $Re = 5 \times 10^3$–4×10^4, for angles of attack $\alpha = 4$, 7, 10, and 13 deg. Consider the vortices formed from the fuselage (main body) of the planform. It is evident that the onset of either a pronounced undulation of the dye marker or an abrupt

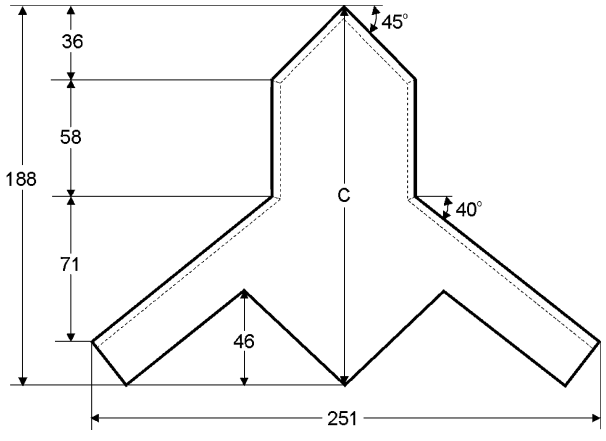

Fig. 1 Model geometry (dimensions in millimeters).

Received 5 November 2003; revision received 9 March 2004; accepted for publication 10 March 2004.

*Research Assistant, Department of Mechanical Engineering and Mechanics, 356 Packard Laboratory, 19 Memorial Drive West. Student Member AIAA.

†Paul B. Reinhold Professor, Department of Mechanical Engineering and Mechanics, 356 Packard Laboratory, 19 Memorial Drive West; dor0@lehigh.edu.

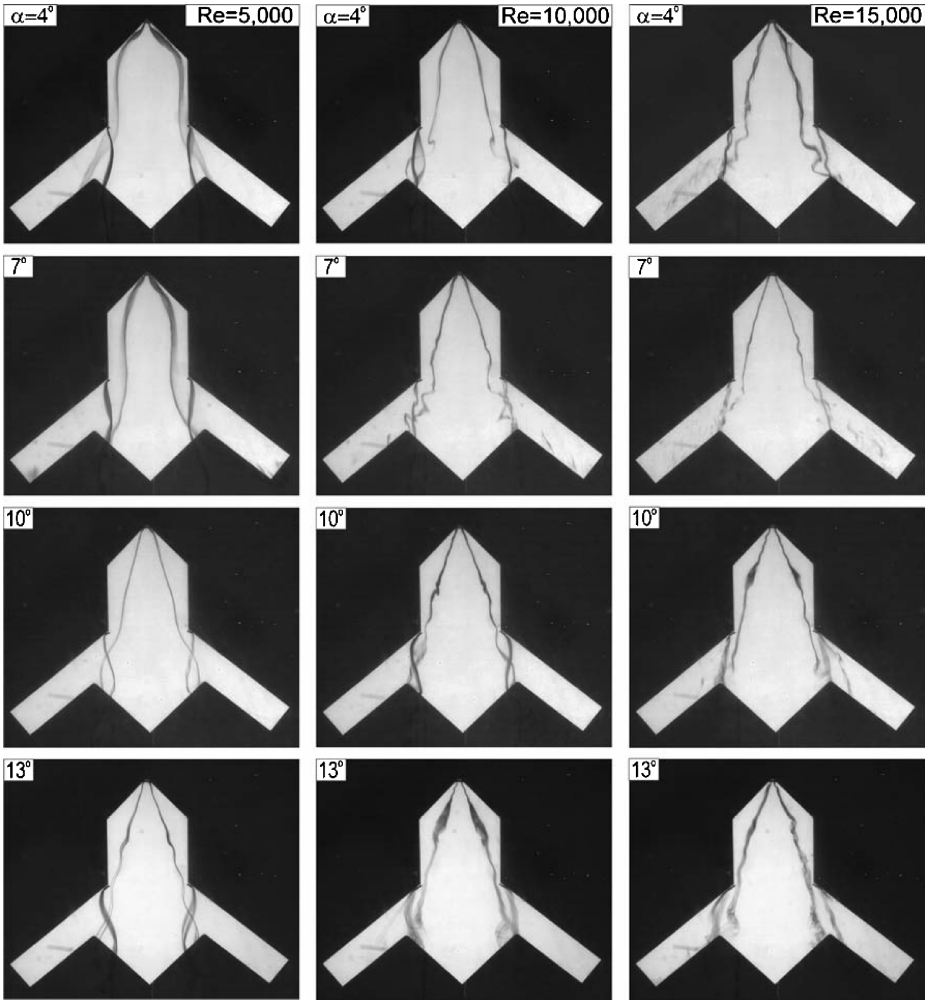

Fig. 2a Effect of Reynolds number *Re* and angle of attack α of UCAV planform on visualized cores of vortices emanating from the fuselage and the wing root.

increase in cross-sectional area of the dye pattern occurs closer to the wing apex for higher values of Reynolds number. Furthermore, at a given value of Reynolds number, these types of substantial disruptions of the dye marker occur closer to the apex of the wing with increasing values of angle of attack α. Another general feature is the degree of interaction of the vortices from the fuselage and the wing root. They generally tend to interact at lower values of Reynolds number, then develop reasonably independently at higher values of Reynolds number. Still another indicator is the angle of inclination, or effective sweep angle, of the centerline of the wing root vortex. This effective sweep angle tends to decrease with increasing Reynolds number.

In the following sections, these observations are addressed in further detail and corresponding plots are provided to define the dependence on Reynolds number.

IV. Vortex Interaction

Consider the range of Reynolds number *Re* and angle of attack α shown in Figs. 2a and 2b. It is evident that, at lower values of Reynolds number, substantial interaction occurs between the fuselage vortex and the wing vortex. At $Re = 5 \times 10^3$, $\alpha = 10$ and 13 deg, vortices are formed form both the apex and wing root regions, and their interaction is clearly evident. At higher values of $Re = 1 \times 10^4$ and 1.5×10^4 the form of the interacting vortices becomes more complex, for example, at $\alpha = 7$ deg, $Re = 1 \times 10^4$. Finally, at the highest values of Reynolds number, the vortices no longer interact. This onset of noninteracting vortices occurs at lower values of Reynolds number for higher values of α. For example, at $\alpha = 13$ deg, $Re = 1 \times 10^4$, intertwining of the vortices no longer occurs, whereas at the lowest angle of attack $\alpha = 4$ deg, a clear indication of noninteraction does not occur until $Re = 3 \times 10^4$.

Figure 3 shows the conditions for the onset of noninteracting vortices in relation to angle of attack α and Reynolds number *Re*. The trend is clearly in accord with the aforementioned observations, that is, as the angle of attack increases, the onset of noninteracting vortices occurs at substantially lower values of Reynolds number.

V. Onset of Pronounced Vortex Instability/ Vortex Breakdown

The onset of vortex breakdown is difficult to define precisely for wings of low sweep angle. As indicated in the numerical and experimental investigations of Gordnier and Visbal[5] and Yaniktepe and Rockwell,[6] a sequence of states of the vortex core involving pronounced undulations, small-scale bubbles, and large-scale breakdown can often occur. As a consequence, it is challenging to define precisely the onset of vortex breakdown, which occurs in a much simpler spiral or bubble mode on a wing of low sweep angle. For our present purposes, we define a location x_b normalized by the chord *C* of the entire planform. The symbol x_b represents the onset of either a pronounced undulation of the vortex core or an abrupt onset of widening of the core.

At $Re = 5 \times 10^3$ for values of α up to 10 deg, the dye markers remain entirely laminar. At $\alpha = 13$ deg, however, pronounced undulation occurs, as indicated in Fig. 4. At $Re = 1 \times 10^4$ the onset of marked undulations moves upstream toward the apex with increasing values of α until, at $\alpha = 13$ deg, a small-scale, bubblelike region forms immediately downstream of the apex. Elements of these patterns of the dye marker are present at $Re = 1.5 \times 10^4$. At higher

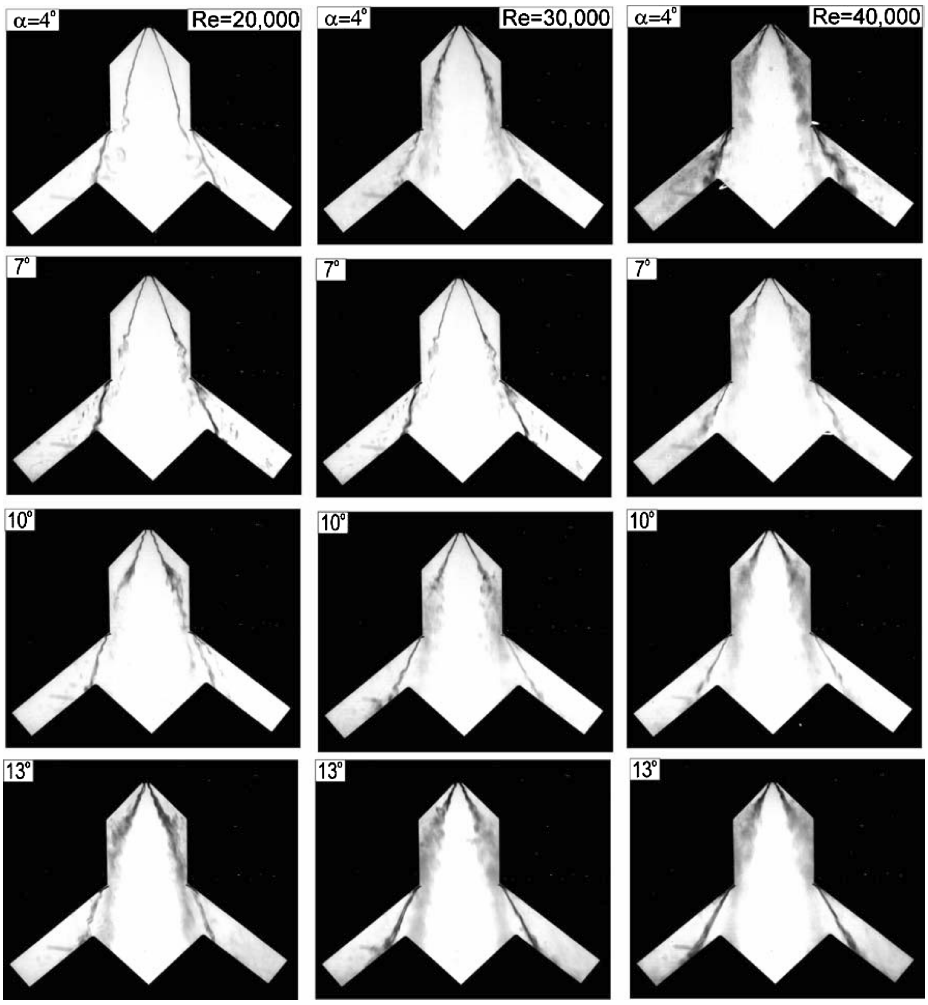

Fig. 2b Effect of Reynolds number *Re* and angle of attack α of UCAV planform on visualized cores of vortices emanating from the fuselage and the wing root.

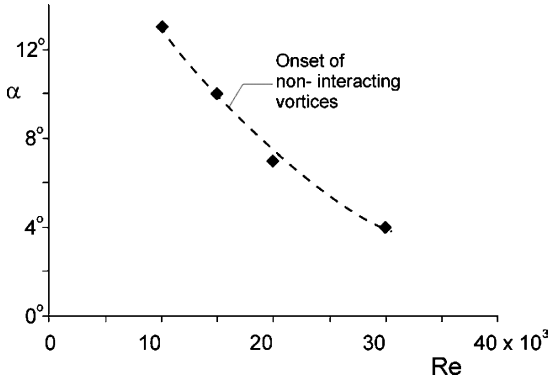

Fig. 3 Onset of noninteracting vortices formed from the fuselage and the wing root in relation to the angle of attack α and Reynolds number *Re* based on chord *C* of planform.

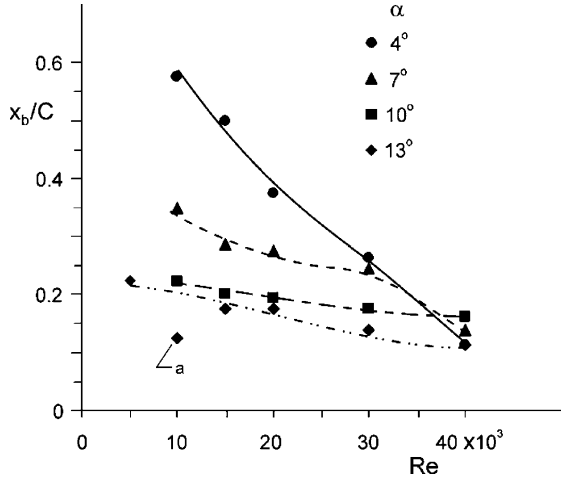

Fig. 4 Location x_b/C of onset of pronounced undulations or breakdown of vortex core as a function of Reynolds number *Re* based on chord of planform.

values from $Re = 2 \times 10^4$ to 4×10^4, depending on the value of α, abrupt widening of the vortex core that involves highly turbulent activity can be discerned. In fact, at the highest value of $Re = 4 \times 10^4$, this abrupt transformation occurs relatively close to the apex for all values of α.

Figure 4 indicates the location x_b/C of the onset of pronounced undulations/breakdown of the vortex core vs Reynolds number *Re* for various values of angle of attack α. The uncertainty of the breakdown location is within 2.9% of the chord *C*. At $\alpha = 10$ and 13 deg, only mild changes of x_b/C are evident over the range of Reynolds number. The outlier point *a* corresponds to the abrupt onset of the small-scale bubble at $\alpha = 13$ deg and $Re = 1 \times 10^4$. At $\alpha = 7$ deg, larger variations are evident, and at $\alpha = 4$ deg, very substantial changes in x_b/C occur for increase of Reynolds number. Whereas asymptotic values of x_b/C are clearly evident for $\alpha = 10$ and 13 deg, this is not the case for smaller values of α, especially at $\alpha = 4$ deg. Note, however, that at the highest Reynolds number $Re = 4 \times 10^4$, the onset of pronounced undulations/breakdown has progressed to a location relatively close to the tip of the apex region, so that

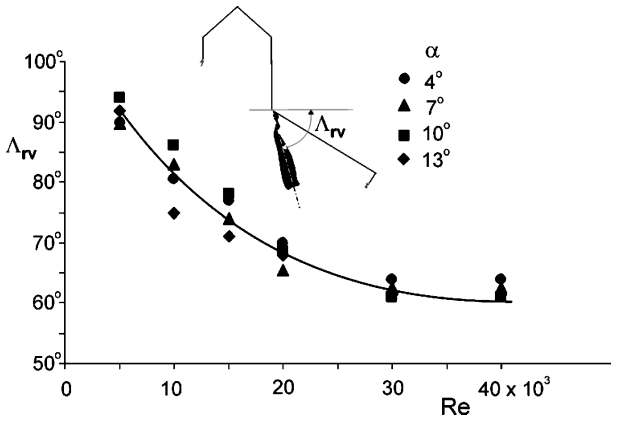

Fig. 5 Effective sweep angle Λ_{rv} of vortex formed from wing root as a function of Reynolds number *Re* based on chord *C* of planform.

further increases in Reynolds number are likely to yield only small decreases in x_b/C.

In the foregoing, emphasis has been on the onset of pronounced undulations/breakdown for the vortices emanating from the apex of the planform. It is, however, possible to discern the onset of vortex breakdown of the wing root vortex at higher values of Reynolds number. For example, see $\alpha = 7$ deg, $Re = 3 \times 10^4$. This onset of breakdown at $\alpha = 7$ deg appears to move closer to the wing root for an increase of Reynolds number *Re* to 4×10^4.

VI. Angles of Inclination of Wing Root and Apex Vortices

Another indicator of the effect of Reynolds number is the angle of inclination of the vortex emanating from the wing root. It is possible to determine an effective sweep angle Λ_{rv} of this vortex core, as defined in the schematic of Fig. 5. As indicated, it is the angle between a line drawn through the center of the vortex core (or, in cases where the core exhibits a spiral, through the center of the spiral) and a line that is perpendicular to the plane of symmetry of the wing. In other words, this effective sweep angle is equivalent to the definition of sweep angle of the leading edge of a delta wing. The dye images of Figs. 2a and 2b indicate that, at lower values of Reynolds number extending up to $Re = 2 \times 10^4$, the value of the effective sweep angle Λ_{rv} varies substantially, whereas at $Re = 3 \times 10^4$ and 4×10^4 little change is evident, indicating that an asymptotic value has been attained. The plot of Fig. 5 clarifies this trend, and emphasizes that the angle Λ_{rv} is a mild function of angle of attack α. This observation contrasts with the strong effect of α on the onset of pronounced undulations/breakdown x_b/C indicated in Fig. 4. Regarding the values of sweep angle of the vortices from the apex of the wing, it is predominantly a function of Reynolds number. At a given Reynolds number, over the values of $\alpha = 4$–13 deg, the range of values of sweep angle Λ_{av} of the apex vortex are as follows. For $Re = 10{,}000$, $14^\circ \le \Lambda_{av} \le 17^\circ$; for $Re = 15{,}000$, $15^\circ \le \Lambda_{av} \le 20^\circ$; for $Re = 20{,}000$, $17.5^\circ \le \Lambda_{av} \le 20^\circ$; for $Re = 30{,}000$, $21^\circ \le \Lambda_{av} \le 23^\circ$; and for $Re = 40{,}000$, $27.5^\circ \le \Lambda_{av} \le 32^\circ$.

VII. Conclusions

This Reynolds number dependence of the vortex patterns on a representative UCAV planform, which is distinguished by small sweep angles, can be defined in terms of the onset of pronounced instability/abrupt breakdown of the vortices from the apex of the main body, the effective sweep angle of the vortices from the wing root, and the degree of interaction of the vortices from the apex and the wing root. At relatively low angle of attack, the onset of pronounced instability/breakdown is highly sensitive to Reynolds number, whereas at relatively high angle of attack, it is much less sensitive. The effective sweep angle of the wing root vortex is only a mild function of angle of attack; it is predominantly a function of Reynolds number and tends toward an asymptotic value at high Reynolds number. The Reynolds number at which the vortices from the apex and the wing root cease to interact decreases substantially with a decrease in angle of attack.

Acknowledgments

The authors gratefully acknowledge the support of the U.S. Air Force Office of Scientific Research, under Grant F49620-02-1-0061, monitored by John Schmisseur.

References

[1]Hebbar, S. K., Platzer, M. F., and Fritzelas, A. E., "Reynolds Number Effects on the Vortical-Flow Structure Generated by a Double-Delta Wing," *Experiments in Fluids*, Vol. 28, 2000, pp. 206–216.

[2]Verhaagen, N. G., "Effects of Reynolds Number on Flow over 76/40-Degree Double-Delta Wings," *Journal of Aircraft*, Vol. 39, No. 6, 2002, pp. 1045–1052.

[3]Visser, K. D., and Washburn, A. E., "Transition Behavior on Flat Plate Delta Wings," AIAA Paper 94-1850, June 1994.

[4]Verhaagen, N. G., Jenkins, L. N., Kern, S. B., and Washburn, A. E., "A Study of the Vortex Flow over a 76/40-deg Double-Delta Wing," AIAA Paper 95-0650, Jan. 1995.

[5]Gordnier, R. E., and Visbal, M. R., "Higher-Order Compact Difference Scheme Applied to the Simulation of a Low Sweep Delta Wing Flow," AIAA Paper 2003–0620, Jan. 2003.

[6]Yaniktepe, B., and Rockwell, D., "Flow Structure in Regions of Vortex Breakdown and Stall on a Delta Wing of Low Sweep Angle," *AIAA Journal*, Vol. 42, No. 3, 2004, pp. 513–523.

Suppression of Wing Rock Using Artificial Neural Networks and Fuzzy Logic Controller

A. G. Sreenatha* and P. P. Wong†
University of New South Wales,
Canberra, Australian Capital Territory 2600, Australia
and
J. Y. Choi‡
Seoul National University,
Seoul 151-600, Republic of Korea

Introduction

THE dynamics of single delta free to roll model at high angles of attack show a nonlinear phenomenon known as wing rock. Wing rock is a complicated aerodynamic phenomenon, characterized by self-induced limit-cycle roll oscillations. Aerodynamic suppression, the suppression of wing rock by the direct control and manipulation of leading-edge vortices, has demonstrated to be effective in controlling wing rock in slender delta wings.[1–5] A particular type of aerodynamic suppression known as recessed angle spanwise blowing (RASB), has been implemented by Sreenatha and Ong[5] via a simple rule-base controller. Experimental results in the wind tunnel revealed the effectiveness of RASB at one angle of attack and freestream velocity. Currently, the mathematical

Received 4 December 2003; revision received 24 February 2004; accepted for publication 24 February 2004.

*Senior Lecturer, School of Aerospace, Civil and Mechanical Engineering, University College, Northcott Drive.

†Student, School of Aerospace, Civil and Mechanical Engineering, University College, Northcott Drive.

‡Associate Professor, School of Electrical and Computer Engineering, Kwanak P.O.Box 34.